Flow Past a Short Cylinder on a Beta Plane with Side Walls

By J. R. Bruzzese,
Dept. of Aerospace Engineering
The Ohio State University
Columbus, Ohio 43210

Geophysical fluid flows over short obstacles in mid-latitude systems experience disturbances due to the Coriolis force created by the rotation of the earth. These Rossby waves radiate downstream with a wave length several times the diameter of the obstacle. Previous studies at The Ohio State University have examined this phenomenon using a beta-plane approximation which linearizes the Coriolis force about the point of the obstacle. The most recent of these is M. L. Bryant and M. R. Foster, 2003.

The findings of these studies could not be validated through laboratory testing since they were computed for an open (boundaryless) flow. The effects of the side walls necessary for a controlled test were unknown. Here we numerically reevaluate the previously considered problem with the added the effect of sidewalls. With its results, the physical problem modeled can be easily reproduced to confirm the study's findings.

1. Introduction

Flow past a cylinder in a rotating channel with the beta plane effect was modeled. This setup is shown in figure 1.1.

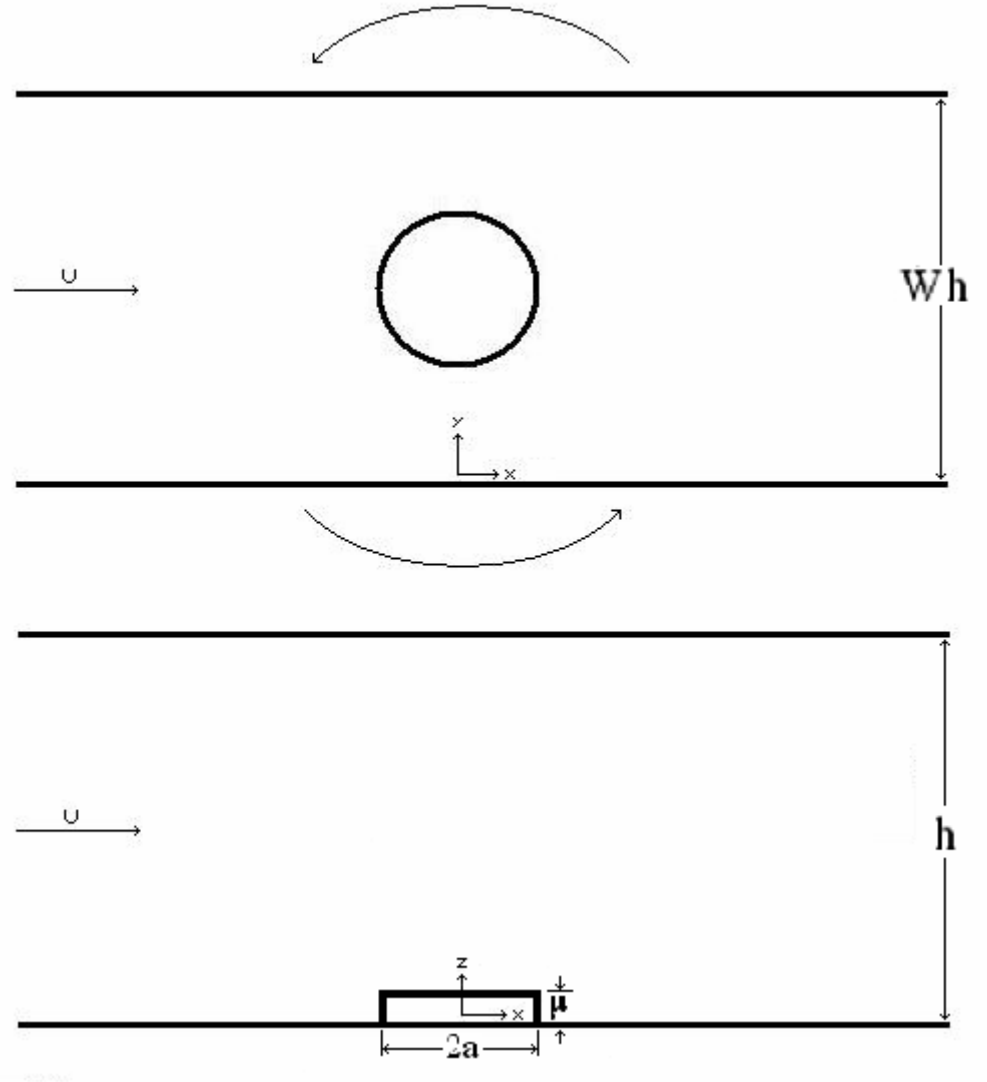

Figure 1.1: Model Setup

The Navier-Stokes equations for a rotating frame of reference are reduced by means of an asymptotic method to a two dimensional solution for which the stream function is calculated. This stream function is expressed as an infinite sine series which has been truncated to include the first four terms. The coefficients of that series are found using second order accurate finite difference schemes. The streamline plots produced can be validated through a qualitative comparison with experimental results published in Boyer and Davies (1983).

2. Formulation

2.1 Governing Equations

The governing equations for the flow considered here are the Navier-Stokes equations written for a rotating reference frame. Nondimensionalized with the Rossby Number (ε) and the Ekman Number (E), they are,

$$\varepsilon \frac{D\mathbf{u}}{Dt} + 2\mathbf{k} \times \mathbf{u} + \nabla p = E\nabla^2 \mathbf{u}$$

$$\nabla \cdot \mathbf{u} = 0$$

where,

$$\varepsilon \equiv \frac{U}{\Omega h},$$

$$E \equiv \frac{\nu}{\Omega h^2},$$

and **u** is the dimensionless velocity vector and ν is the kinematic viscosity.

2.2 Assumptions

The flow is taken to be incompressible. It is necessary that there be straight streamlines on the side walls of the channel. We will see that u=O(1), v=O(1), and w=O(ε). In order to match typical experimental conditions, $\varepsilon=O(10^{-2})$ and $E=O(10^{-4})$. This leads to an asymptotic expansion where we approximate the solution for a small ε by

$$\mathbf{u} = \mathbf{u}_0 + \varepsilon \mathbf{u}_1 + \varepsilon^2 \mathbf{u}_2 + \ldots,$$

$$p = p_0 + \varepsilon p_1 + \varepsilon^2 p_2 + \ldots.$$

The dimensional Coriolis force on a rotating planet is given by

$$2cU(\mathbf{k} \times \mathbf{u}).$$

The Beta plane approximation linearizes the variation in Coriolis force due to lateral motion about a given latitude

$$c = 2\Omega \sin\phi \approx 2\Omega \sin\phi_0 + \frac{2\Omega \cos\phi_0}{R} y,$$

where Ω is the axial velocity of the earth, R is the radius of the earth, and ϕ is the latitude. The governing equation becomes

$$\varepsilon \frac{D\mathbf{u}}{Dt} + 2(1 + \beta y \varepsilon)\mathbf{k} \times \mathbf{u} + \nabla p = E\nabla^2 \mathbf{u},$$

where

$$\beta_0 = \frac{h\cos(\phi_0)}{\varepsilon R\sin(\phi_0)} = \mathrm{O}(1).$$

2.3 Simplifications

The O(1) equations simplify to

$$2\mathbf{k}\times\mathbf{u}_0 + \nabla p_0 = 0$$

$$\nabla\cdot\mathbf{u}_0 = 0\,.$$

What emerges from these equations is

$$w_0 = 0\,,$$

$$\frac{\partial u_0}{\partial z} = \frac{\partial v_0}{\partial z} = \frac{\partial p_0}{\partial z} = 0\,. \tag{2.3.1}$$

The O(ε) equations simplify to

$$u_0\frac{\partial u_0}{\partial x} + v_0\frac{\partial u_0}{\partial y} - 2v_1 - 2\beta_0 y v_0 + \frac{\partial p}{\partial x} = 0\,,$$

$$u_0\frac{\partial v_0}{\partial x} + v_0\frac{\partial v_0}{\partial y} + 2u_1 + 2\beta_0 y u_0 + \frac{\partial p}{\partial y} = 0\,,$$

$$\nabla\cdot\mathbf{u}_1 = 0\,.$$

The O(ε) *x* and *y* momentum equations are differentiated and subtracted to get

$$(\mathbf{u}_0\cdot\nabla)(-\zeta_0) + 2\frac{\partial w_1}{\partial z} - 2\beta_0 v_0 = 0\,. \tag{2.3.2}$$

This equation is differentiated with respect to z, using equation 2.3.1 to give

$$\frac{\partial^2 w_1}{\partial z^2} = 0\,. \tag{2.3.3}$$

This result shows that w_1 is linear with respect to z. Boundary conditions require the flow to be parallel to the boundaries. At the top surface (z=1),

$$w_1 = 0\,,$$

and at the bottom surface (z=0),

$$w_1 = \mu\mathbf{u}_0\cdot\nabla f\,.$$

Given these two w_1's, equation 2.3.3 gives

$$\frac{\partial w_1}{\partial z} = -\mu\mathbf{u}_0\cdot\nabla f\,.$$

Equation 2.1.2 can be rewritten as

$$(\mathbf{u}_0 \cdot \nabla)[\varsigma_0 + 2\mu f + 2\beta_0 y] = 0 .$$

This allows for the formulation of the stream function

$$\varsigma_0 + 2\mu f + 2\beta_0 y = F(\Psi_0) = 2\beta_0 \Psi_0 , \tag{2.3.4}$$

where

$$\psi = y ,$$

$$\psi' = \sum_{n=1}^{N} A_n \sin(\frac{n\pi y}{W}) ,$$

$$\Psi_0 = \psi + \psi' .$$

Equation 2.3.4 can be simplified using

$$\varsigma_0 + 2\mu f + 2\beta_0 y = 2\beta_0(\psi + \psi') ,$$

$$2\beta_0 y = 2\beta_0 \psi ,$$

$$\varsigma_0 = -\nabla^2 \psi' .$$

This evaluation of $F(\Psi_0)$ assumes that all streamlines originate upstream. So, solutions with closed stream lines much be discarded. These results lead to

$$\nabla^2 \psi' + 2\beta_0 \psi' = 2\mu f ,$$

$$\sum_{n=1}^{N} [\frac{\partial^2}{\partial x^2} A_n + (\lambda^2 - \frac{n^2\pi^2}{W^2}) A_n] \sin(\frac{n\pi y}{W}) = 2\mu f ,$$

where W is the dimensionless width of the channel. Multiplying by $\sin(\frac{m\pi y}{W})$ and integrating yields

$$\sum_{n=1}^{N} [\frac{\partial^2}{\partial x^2} A_n + (\lambda^2 - \frac{n^2\pi^2}{W^2}) A_n] \int_0^1 \sin(\frac{n\pi y}{W}) \sin(\frac{m\pi y}{W}) dy = \int_0^1 2\mu f \sin(\frac{m\pi y}{W}) dy .$$

This is then simplified to

$$\frac{\partial^2}{\partial x^2} A_n + (\lambda^2 - \frac{n^2\pi^2}{W^2}) A_n = 4 \int_0^1 \mu f \sin(\frac{n\pi y}{W}) dy . \tag{2.3.5}$$

It can be shown that the integral on the right side of this equation is zero for any even n for a symmetrical obstacle in the center of the channel. This leads to a trivial solution. For this reason, only odd n's need to be further considered.

3. Numerical Method

3.1 Finite Difference Schemes

There are two distinct sorts of solutions. For $\lambda < \frac{n\pi}{W}$, the solution to the differential equation has exponential decay. For this case, a second order accurate central differencing scheme is used to give

$$\frac{A_{n_{i+1}} - 2A_{n_i} + A_{n_{i+1}}}{dx^2} + \left(\lambda^2 - \frac{n^2\pi^2}{W^2}\right)A_{n_i} = G_i .$$

For $\lambda > \frac{n\pi}{W}$, the solutions are oscillatory. The radiation condition for these Rossby waves is that they may only exist downstream only. For this reason, a second order accurate backwards difference scheme must be employed to give

$$\frac{-A_{n_{i-3}} + 4A_{n_{i-2}} - 5A_{n_{i-1}} + 2A_{n_i}}{dx^2} + \left(\lambda^2 - \frac{n^2\pi^2}{W^2}\right)A_{n_i} = G_i . \qquad (3.1.1)$$

3.2 Numerical Damping

The finite difference scheme for the wave case ($\lambda > \frac{n\pi}{W}$) experiences artificial downstream damping with a magnitude proportional to the step size taken. This is demonstrated in figures 3.2.1-3.2.3 where the first four terms are plotted.

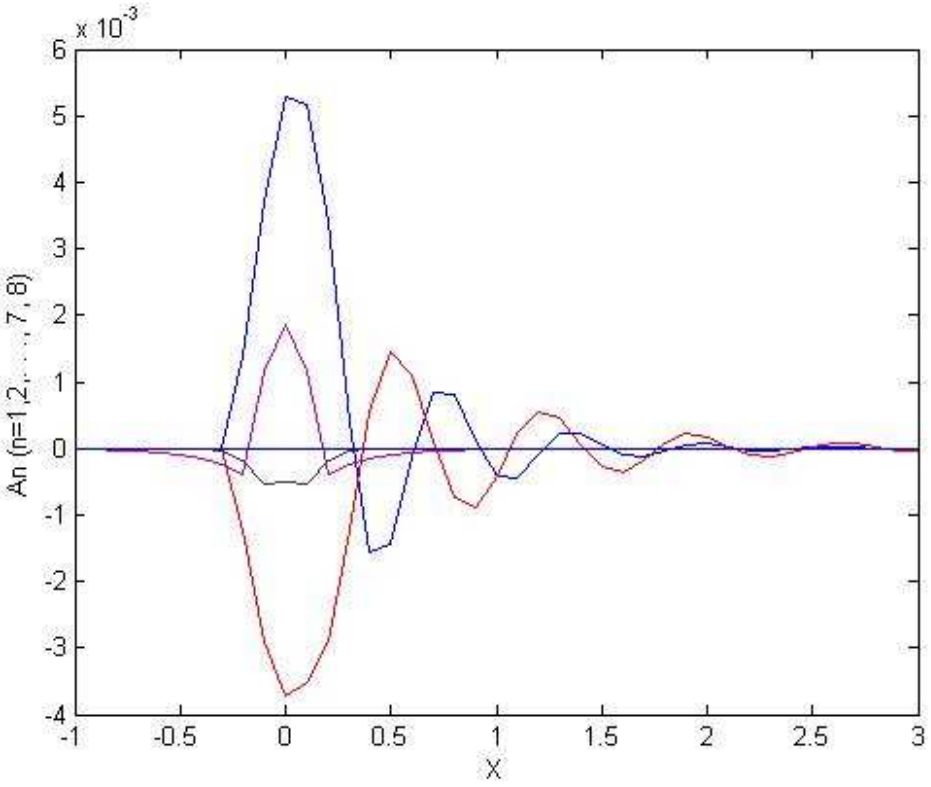

Figure 3.2.1: A_n for $\mu=1$, $\lambda=15$, $a=0.25$, $W=1$, $\Delta x=0.1$

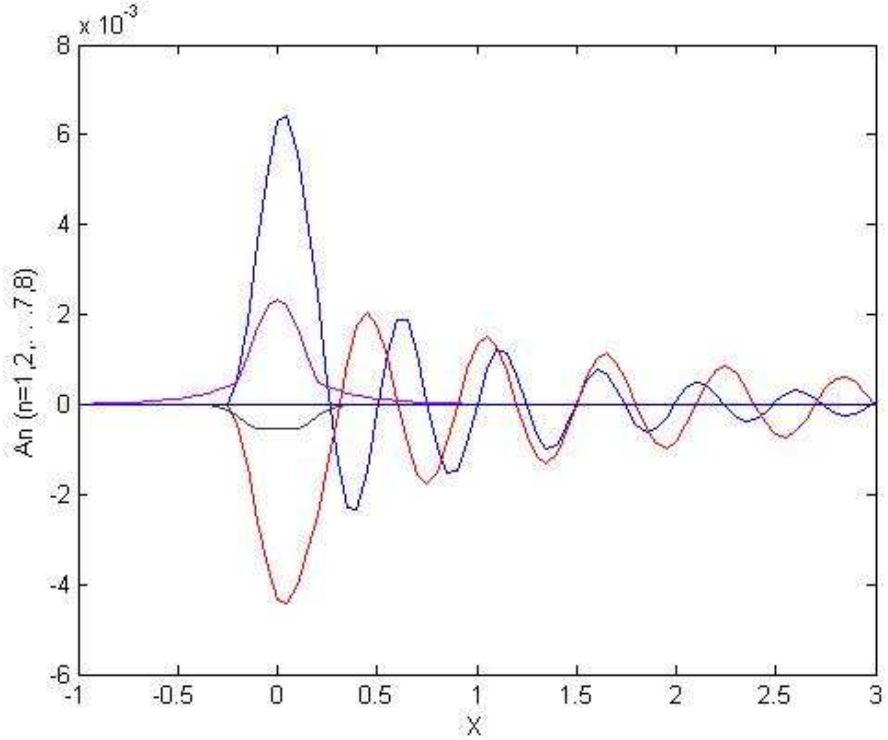

Figure 3.2.2: A_n for $\mu=1$, $\lambda=15$, $a=0.25$, $W=1$, $\Delta x=0.05$

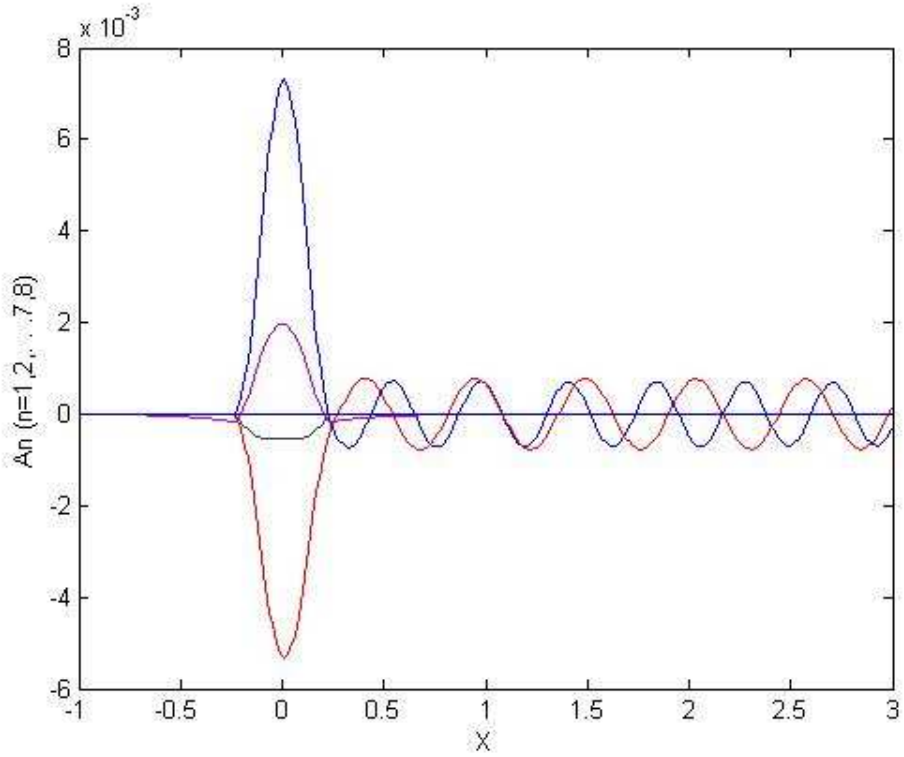

Figure 3.2.3: A_n for $\mu=1$, $\lambda=15$, $a=0.25$, $W=1$, $\Delta x=0.01$

It can be seen that this damping gets much smaller as Δx becomes small. The damping effects displayed graphically can be confirmed by an analytical solution of equation 3.1.1. This determines the step size necessary to produce accurate results ($x_{max}\,\Delta x<10^{-2}$ is required).

3.3 Number of Terms

As n goes to infinite, the integral on the right side of equation 2.3.5 goes to zero. Knowing this, the solution can be truncated to include only the first four terms. This number would need to be increased to capture all the modes for greater values of λ, but four is enough for all cases considered here. The comparison in figure 3.3.1 shows the error induced by this truncation. The figure on the left shows the first 4 terms in the series while the figure on the right shows the first 6 terms. As can clearly be seen, the effect of the 5^{th}, 6^{th}, and all subsequent terms is negligible.

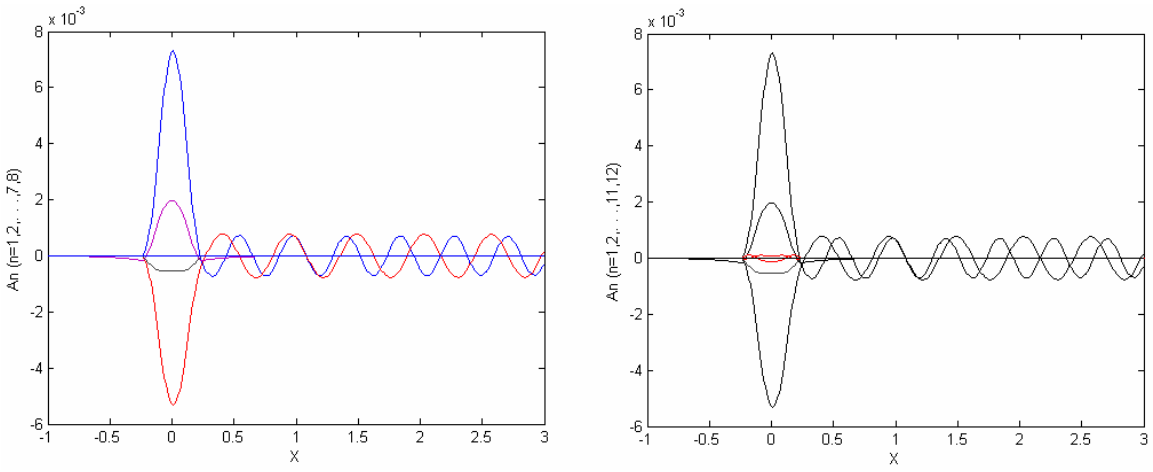

Figure 3.3.1: Effect of Series Truncation

3.4 Summation of the Stream Function

Having solved for A_n, the stream function at any (i,j) can then be computed using

$$\psi'_{i,j} = \sum_{n=1}^{N} A_{n_i} \sin(\frac{n\pi y_j}{W}),$$

$$\psi_{i,j} = y_j,$$

$$\Psi_{i,j} = \psi_{i,j} + \psi'_{i,j}.$$

4. Results and Conclusions

4.1 Streamline Plots

As can be seen in figure 4.1.1, no waves are present for $\lambda < \frac{n\pi}{W}$.

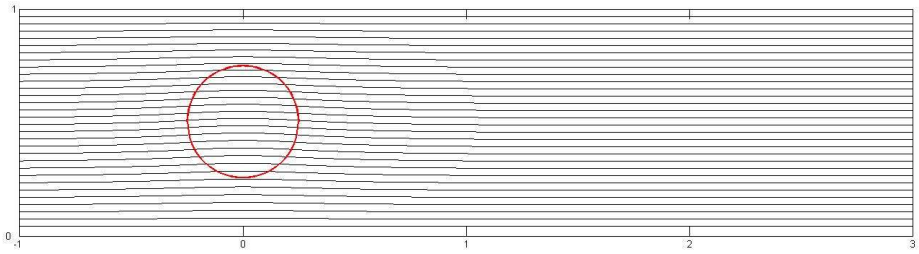

Figure 4.1.1: No Wave Case (μ=1, λ=2, a=0.25, W=1)

Figure 4.1.2 shows that widening the channel will produce waves for values of λ that the narrower channel would not.

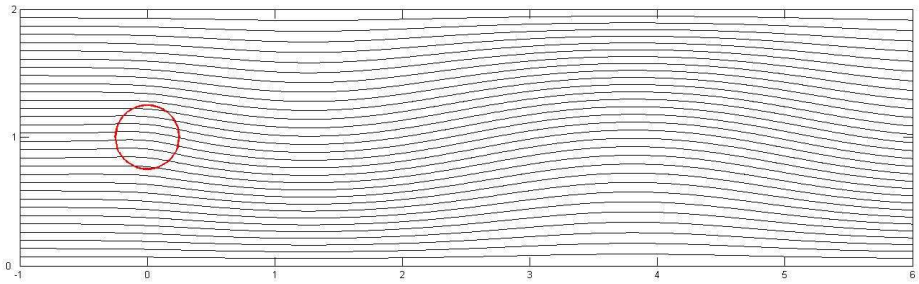

Figure 4.1.2: No Wave Case (μ=1, λ=2, a=0.25, W=2)

Figure 4.1.3 shows the Rossby waves downstream. This figure is used as the basis of comparison for the remaining figures.

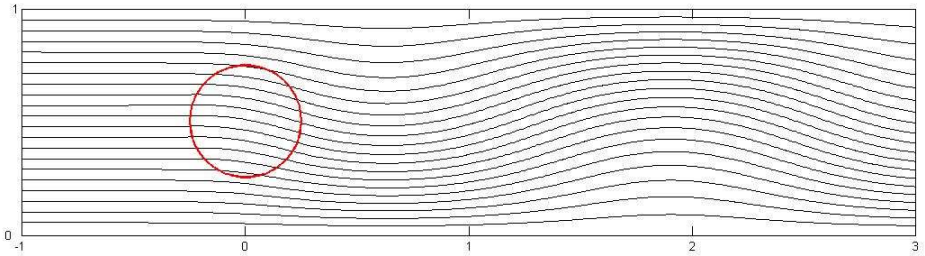

Figure 4.1.3: Wave Case (μ=1, λ=4, a=0.25, W=1)

Figure 4.1.4 shows that increasing λ decreases the wavelength of the expressed mode.

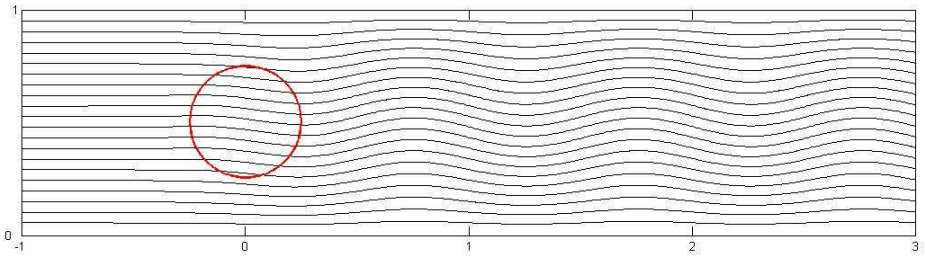

Figure 4.1.4: Shorter Wave Length (μ=1, λ=7, a=0.25, W=1)

Figure 4.1.5 shows that increasing μ increases the amplitude of the waves. This can be seen in equation 2.1.5, as the forcing function on the right side is directly proportional to μ. Intuitively, increasing the obstacle size should increase its effect on the flow.

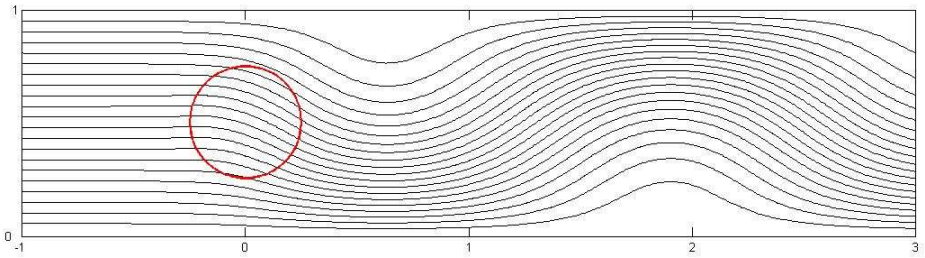

Figure 4.1.5: Increased Amplitude (μ=2, λ=4, a=0.25, W=1)

Figure 4.1.6 shows that decreasing the cylinder radius decreases the amplitude of the waves. Intuitively, this decreasing the obstacle size should decrease its effect on the flow, but this is harder to see in the equations, as it is expressed in reduced bounds of the integral on the right side of equation 2.3.5.

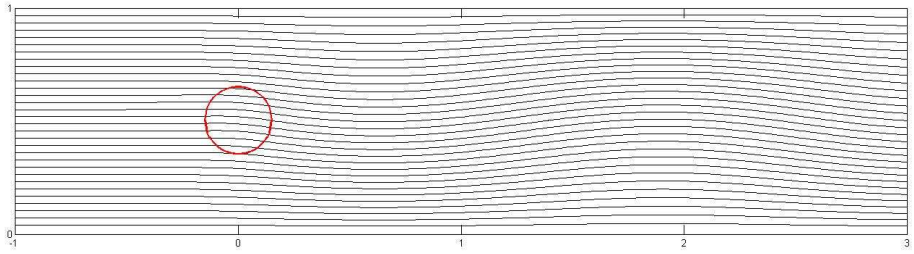

Figure 4.1.6: Reduced Amplitude (μ=1, λ=4, a=0.15, W=1)

Figure 4.1.7 shows an interference pattern of two modes of Rossby waves.

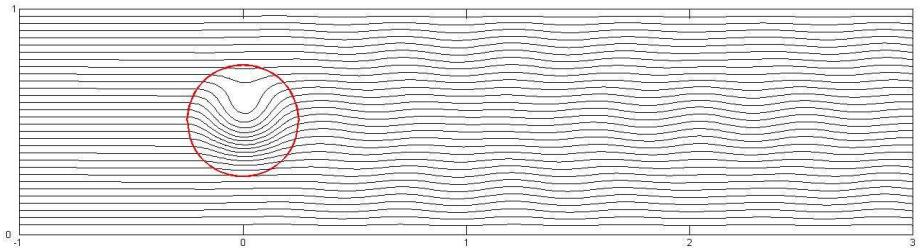

Figure 4.1.7: Interference Pattern (μ=10, λ=15, a=0.25, W=1)

4.2 Model Failure

Model failure can occur in two ways. For sufficiently large values of μ and a, the flow can become so disturbed that eddies appear in the form of closed streamlines. This invalidates the assumption made in equation 2.3.4 that all streamlines originate upstream. The second case of model breakdown occurs when λ is sufficiently close to $\frac{n\pi}{W}$. For this case, equation 3.1.1 becomes

$$\frac{-A_{n_{i-3}} + 4A_{n_{i-2}} - 5A_{n_{i-1}} + 2A_{n_i}}{dx^2} = G_i .$$

A_n diverges for x>a which creates a large open streamline on the downstream border. Among other issues, this also violates the assumption made in equation 2.3.4.

4.3 Conclusions

The number of modes of Rossby waves and the wavelength of those modes is determined

by $\lambda - \frac{n\pi}{W}$. The amplitude of the waves is determined primarily by the size of the obstacle (μ and a). The results obtained here were qualitatively similar to those displayed in Boyer and Davies (1983), but a rigorous quantitative comparison was not able to be conducted. Artificial damping is introduced through the numerical scheme used, and this damping determines the necessary step size. Different finite difference schemes are necessary for wave and non-wave cases to force the radiation condition of downstream waves only. Model failure can occur for large values of μ and a and when λ is sufficiently close to $\frac{n\pi}{W}$.

5. References

M.L. Bryant and M.R. Foster, *Private Communication* (2003)

Polzin, K.A., Angelats, M. and Foster, M.R., "Rotating flow past a short, sliced cylinder at finite Rossby number," *Geophys. Astrophys. Fluid Dynamics* **95**, 67 (2001)

Boyer, D.L. and Davies, P.A., "Laboratory studies of orographic effects in rotating and stratified flows," *Ann. Rev. Fluid Mech.* **32**, 165 (2000)

Boyer, D.L. and Davies, P.A., "Rotating flow past disks and cylindrical depressions," *Journal of Fluid Mech.* **141**, 67 (1983)

Boyer, D.L. and Davies, P.A., "Flow past a circular cylinder on a beta plane," *Philos Trans. R. Soc. London* **306**, 33 (1982)

A special thanks to Dr. Michael R. Foster for helping so extensively on this project.